Journal of the European Ceramic Society **19** (1999) 847–851

PII: S0955-2219(98)00329-X
0955-2219/99/$ - see front matter

Structural and Electrical Characterisation of Silica-containing Yttria-stabilised Zirconia

C. C. Appel† and N. Bonanos*

Materials Research Department, Risø National Laboratory, DK-4000 Roskilde, Denmark

Abstract

Zirconia stabilised by yttria has a high oxide ion conductivity at high temperature and, therefore, is currently used as electrolyte in Solid Oxide Fuel Cells. Silica is normally avoided in this material because formation of amorphous silica phases along the grain boundaries causes an increased grain boundary impedance. The present study examines the effect of SiO_2 and SiO_2 with Mn-oxide on the structure and resistivity of yttria stabilised zirconia electrolyte materials. During fabrication of Solid Oxide Fuel Cells, Mn readily diffuses from the manganite-based cathode into the electrolyte. It is shown that a grain boundary phase which causes an insulating layer in the grain boundaries is formed when both SiO_2 and Mn-oxide coexist in the samples, whereas such effects are much less pronounced when only SiO_2 is present. © *1999 Elsevier Science Limited. All rights reserved*

Keywords: SOFC, grain boundaries, electron microscopy.

1 Introduction

Zirconia stabilised with yttria (YSZ) is the material currently used as electrolyte in Solid Oxide Fuel Cells (SOFC). The highest oxide ion conductivity at 1000°C is found for ZrO_2 with 8 mol% Y_2O_3.[1] While high purity materials are generally required for the SOFC applications, the use of powders with minor impurities such as SiO_2 would significantly reduce costs. It is, therefore, important to know the effect of small amounts of silica on the structure and on the electrical properties of YSZ, especially in the presence of other elements introduced during fuel cell fabrication.

*To whom correspondence should be addressed.
†Present address: Geological Survey of Denmark and Greenland, Department of Geochemistry, DK-2400 Copenhagen NV, Denmark.

Depending on the thermal history of the zirconia, the silica will form an amorphous film along the grain boundaries or concentrate in the triple points. It is well established that the presence of an amorphous silica phase at grain boundaries causes increased grain boundary impedance. Moreover, the silica phase has been shown to concentrate yttrium with respect to zirconium,[2,3] and this also adversely affects the electrical properties of the stabilised zirconia.

It is known that Mn may diffuse from the cathode material into the electrolyte during fabrication and operation of an SOFC.[4] Mn has been shown to cause grain growth in cubic YSZ[5] and to stabilise the cubic phase of zirconia, since its addition causes disappearance of weak diffraction spots due to tetragonal phase, as observed on micrographs of pure YSZ[6] obtained in the transmission electron microscope. Therefore the effect of Mn on the structure and conductivity of YSZ with impurities of silica is very important to know.

2 Sample Preparation and Experimental Techniques

A commercial Tosoh powder of yttria stabilised zirconia of Y_2O_3 content 7·9 mol% (13·6 wt%) was used for sample preparation. Some of the powder was mixed with SiO_2 by ball milling and the resulting powders were tape cast by in-house established techniques. The tapes were sintered at 1350°C for 8 h. A sample containing both Mn and SiO_2 was pressed into a pellet and sintered at the same conditions as the tapes. The Mn was added as $MnCO_3$, which was converted to oxide during heat treatment. The compositions of the examined samples are given in Table 1.

Specimens were ground and polished and examined in a Low Vacuum Scanning Electron Microscope (LVSEM), JEOL LV5310, operated in low vacuum mode or in an Environmental Scanning Electron Microscope (ESEM) Electroscan™. For Transmission Electron Microscopy

Table 1. Nominal composition of the examined samples given in wt% (13·6 wt% ≈ 7·9 mol% Y_2O_3 in ZrO_2)

Sample name	ZrO_2	Y_2O_3	Mn_3O_4	SiO_2
YSZ	86·4	13·6	–	–
YSZSi	86·3	13·6	–	0·1
YSZMnSi	85·2	13·4	1·3	0·1

(TEM) specimens were cut into discs with a diameter of 3 mm. These were ground, polished and thinned by sputtering with Ar-ions to electron transparency in parts of the sample. The TEM was a JEOL 2000FX equipped with Energy Dispersive X-ray Spectrometry (EDS). For impedance spectroscopy, the samples were painted with silver electrodes. Measurements were made in air, in the frequency range 0·1 Hz to 1 MHz using a Solartron 1260 impedance analyser and were converted to units of resistivity based on the dimensions of the sample. A measurement temperature of 300°C was chosen to facilitate resolution of grain and grain boundary relaxations. The software *Equivcrt*[7] was used to analyse the data.

3 Results and Discussion

The secondary electron signal in the ESEM was used to examine the sintered surface of YSZSi [Fig. 1(a)]; 1–2 μm large, angular grains were observed. This is similar to size and form of the grains in YSZ (not shown). In YSZMnSi the grain size is up to 10 μm therefore it was possible on a polished sample to see orientation contrast from the grains by the backscattered electron signal [Fig. 1(b)]. The grains are rounded and the triple points show a dark contrast, signifying either that they are pores, or that they are filled with a light material with a low electron backscattering coefficient. The centre of some of the YSZMnSi grains appears porous while the edges are dense [Fig. 1(b)].

YSZSi was examined by TEM. Crystalline inclusions, some of them faceted, were found in the cubic zirconia grains (Fig. 2). EDS analyses of the inclusions showed that they contain Zr, Y and small amounts of Si. A detailed examination of the inclusions was not made. No glass phase was observed along the grain boundaries. However, the presence of a thin amorphous film along the grain boundaries cannot be excluded because this requires high resolution TEM to be revealed. It was expected that 0·1 wt% SiO_2 in YSZ would produce an amorphous phase at grain boundaries and in triple points as observed earlier in zirconia.[2,3,8] It was therefore as first glance surprising that crystalline silica-containing inclusions were observed. The present observation can be explained by the relatively low sintering temperature used (1350°C). Additionally, the YSZ has a very low concentration of alkali metals such as Na and K, which cause a decrease in the liquidus temperature of SiO_2.

TEM of YSZMnSi revealed cubic YSZ grains with a mottled appearance. Forbidden diffraction spots appeared in the diffraction patterns as

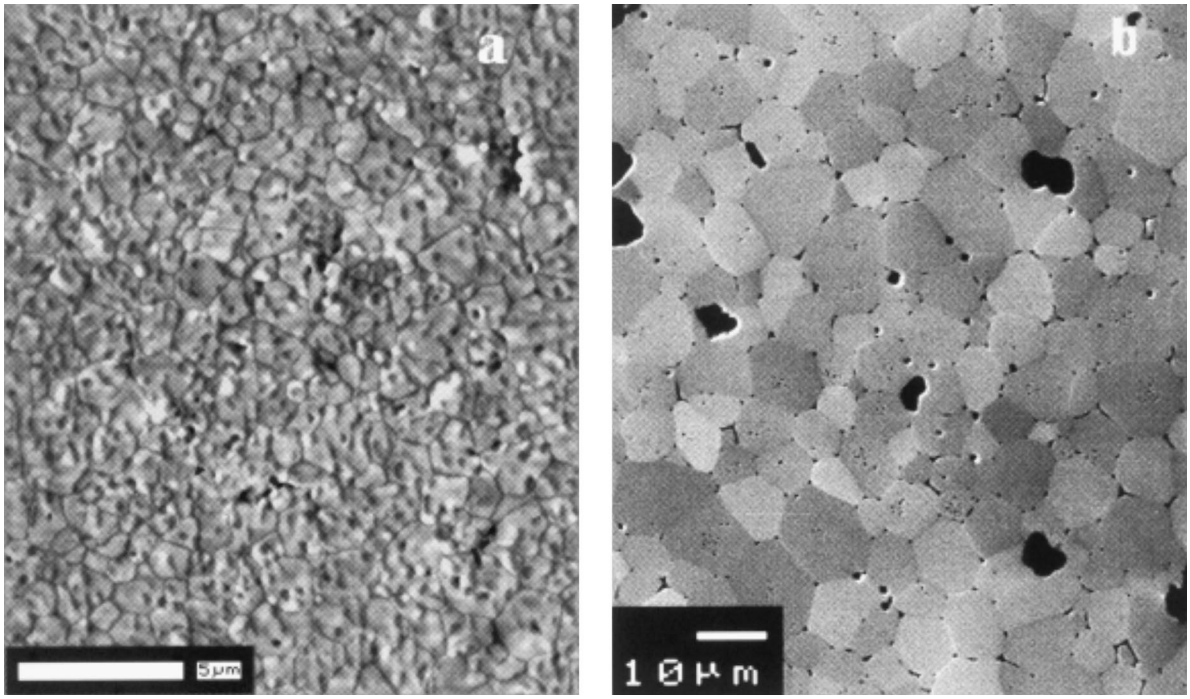

Fig. 1. SEM images of YSZSi and YSZMnSi sintered at 1350°C. (a) Secondary electron image of the surface of YSZSi. 1–2 μm large, angular grains are seen. (b) Backscattered electron image of YSZMnSi. The size of the rounded grains is up to 10 μm.

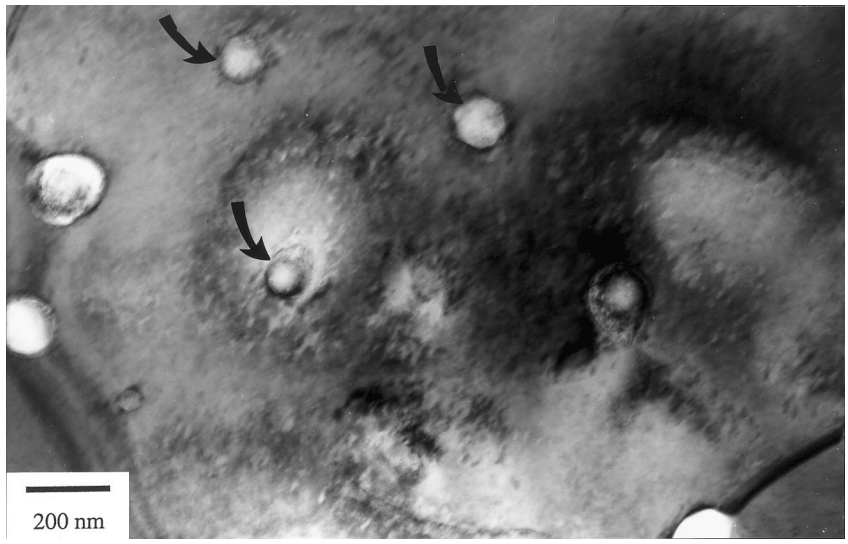

Fig. 2. TEM bright field image of YSZSi. Cubic zirconia grain with silica containing crystalline inclusions. The bright inclusions (marked by arrows) have a size of approximately 100 nm.

observed previously for pure YSZ and for YSZ with 2 mol% Mn ($\approx$1·3 wt% Mn_3O_4) in solid solution.[6] An amorphous phase was observed at the triple points (Fig. 3) and along some of the grain boundaries. The compositions of the cubic zirconia grains and the glassy phases were analysed semi-quantitatively by EDS. The results are presented as ratios between the elements in the zirconia grains and in glass phases (Fig. 4). This is preferable, as point analyses by EDS in TEM often contain information from the surrounding material. Thus a low Si/Zr-ratio shows that the analysis is made in a zirconia grain whereas a high Si/Zr-ratio is observed when the SiO_2 glass phase is analysed. A plot of Y/Zr versus Si/Zr shows that the Y/Zr-ratio of the glass phase is considerably higher than the Y/Zr-ratio of the cubic zirconia [Fig. 4(a)]. Additionally, Mn/Zr in the glassy phase increases with increasing Si/Zr [Fig. 4(b)], this shows that Mn and Y are concentrated in the glass phase in the grain boundaries. 4–5 at% Mn were detected in the glass, whereas less than 1 at% Mn (which is less than the detection limit) was observed in the cubic zirconia grains. Even small amounts of Mn-oxide in SiO_2 cause formation of a liquid phase at temperatures below 1350°C as shown in the 2-component phase diagram, Mn_3O_4-SiO_2.[9] Therefore the presence of both SiO_2 and Mn-oxide in YSZ causes formation of the glass phase and both Mn and Y are concentrated in the amorphous phase.

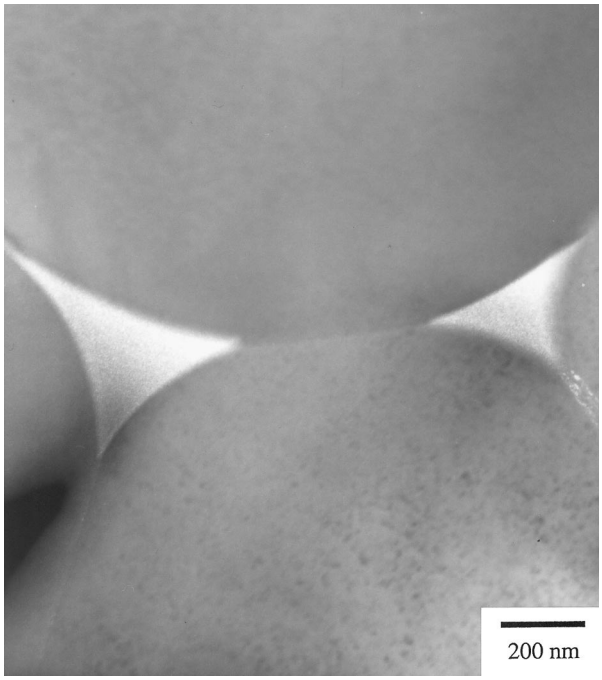

Fig. 3. TEM dark field image of YSZMnSi. Part of the electrons scattered by the amorphous phase are used for the imaging, therefore the glass phase in the triple points and the grain boundaries appears bright.

It is well established that changes in the phase composition and structure of zirconia ceramics are reflected in their impedance spectra.[10,11] The highest frequency relaxation gives the resistivity of the grain interior, while the second highest is related to the structure and resistivity of grain boundary phases.

Figure 5 shows complex resistivity spectra obtained on the three types of sample studied. The spectrum for pure YSZ [Fig. 5(a)] is typical for an optimally sintered zirconia–yttria ceramic, with grain boundaries making a relatively small contribution to the total resistance. The YSZSi sample [Fig. 5(b)] has a slightly increased grain boundary contribution, indicating that a high resistivity phase may be present at the grain boundaries. The grain interior impedance of this sample is slightly smaller than that of YSZ, which is puzzling, bearing in mind that SiO_2 is almost insoluble in YSZ and, therefore, should not affect the bulk

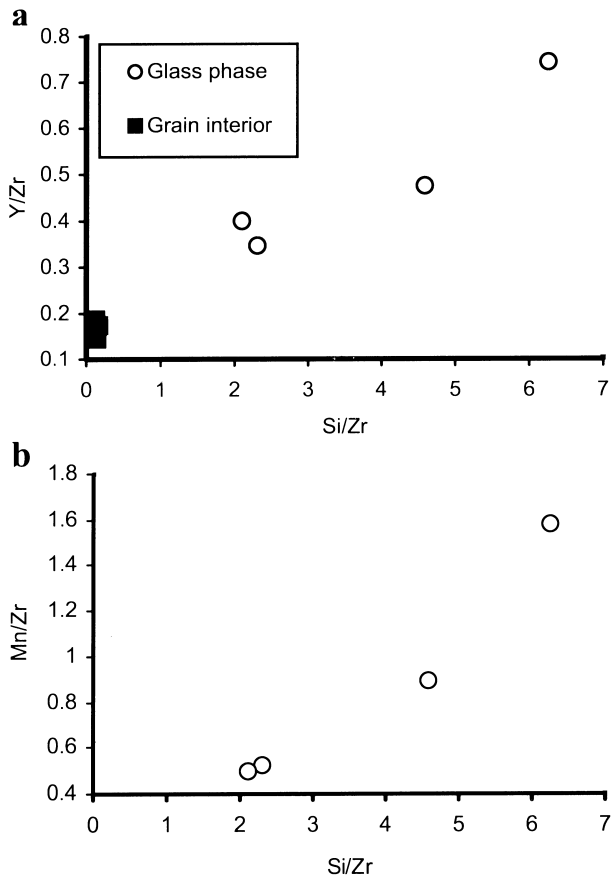

Fig. 4. Variations in element ratios obtained by EDS in YSZMnSi. (a) Y/Zr increases with increasing Si/Zr. (b) Mn/Zr increases with increasing Si/Zr. The plots show that Y and Mn are concentrated in the glass phase.

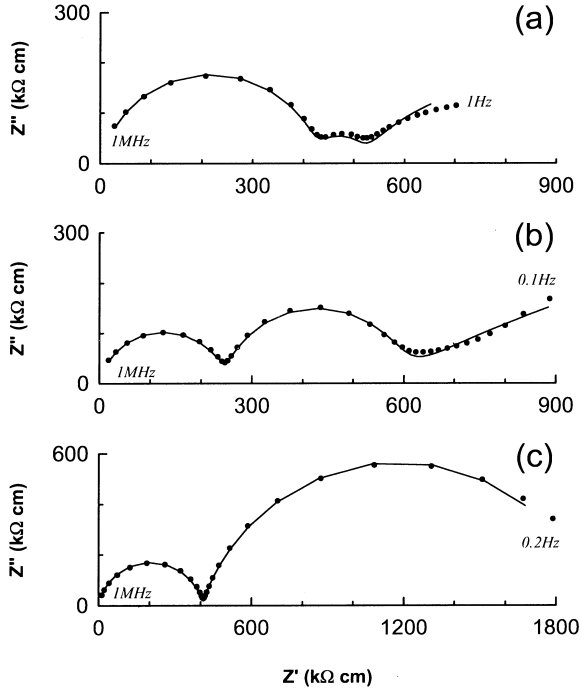

Fig. 5. Complex resistivity spectra obtained at 300°C in air for (a) pure YSZ, (b) YSZSi, (c) YSZMnSi. The latter shows an enlarged grain boundary arc, indicating that the grain boundaries are covered by a phase of poor electrical conductivity.

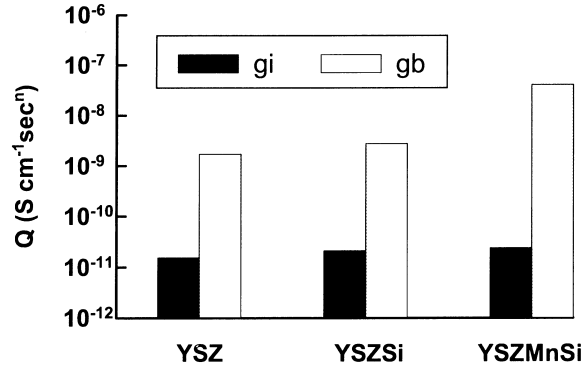

Fig. 6. Values of non-ideal capacitance elements, Q, for grain interior and grain boundary relaxations in the sample examined. The grain boundary value of Q is increased by an order of magnitude when both Mn and Si are present.

properties in any significant way. Finally, the impedance spectrum of YSZMnSi [Fig. 5(c)] shows a greatly enlarged grain boundary arc, indicating that the grain boundaries are highly covered by a phase of poor electrical conductivity.

The grain interior and grain boundary relaxations observed in ceramic electrolytes can be modelled by a circuit of two elements connected in series; $(RQ)(RQ)$ in the notation of Boukamp,[7] where Q represents non-ideal capacitance. The Q-values associated with each element are shown in Fig. 6 for the samples examined. Addition of impurities has little effect on the grain interior capacitance, but the grain boundary capacitance is increased by approximately one order of magnitude when both Mn and Si are present. This indicates that the grain boundaries are covered by an insulating layer, obviously the glassy phase observed by TEM.

4 Conclusion

The effect of SiO_2 and Mn-oxide on structure and electrical properties of YSZ sintered at 1350°C has been studied. Addition of SiO_2 to an otherwise pure YSZ only slightly increased the grain boundary contribution to the total resistivity. Silica containing crystalline particles were observed whereas a continuous grain boundary was not found although the presence of a thin grain boundary film can not be excluded. However, when both Mn-oxide and SiO_2 were added to YSZ amorphous phase is seen in the triple points and along the grain boundaries, moreover the grain morphology changed. The presence of the amorphous phase is reflected in the impedance spectra where the grain boundary contribution to the total resistivity increased considerably due to the insulating grain boundary phase. It has thus been shown how two contaminants commonly found in operating SOFC

change the microstructure and cause degradation of the electrical properties.

Acknowledgements

Specimen preparation was carried out by A.-M. Heie Kjær and H. Paulsen. The work was supported by the EU, contract JOE3-CT95-0005.

References

1. Badwal, S. P. S., Zirconia-based solid electrolytes: microstructure, stability and ionic conductivity. *Solid State Ionics*, 1992, **52**, 23–32.
2. Badwal, S. P. S and Drennan, J., Yttria-zirconia: effect of microstructure on conductivity. *J. Mat. Sci.*, 1987, **22**, 3231–3239.
3. Badwal, S. P. S. and Drennan, J., Grain boundary resistivity in Y-TZP materials as a function for thermal history. *J. Mat. Sci.*, 1989, **24**, 88–96.
4. Clausen, C., Bagger, C., Bilde-Sørensen, J. B. and Horsewell, A., Microstructural and microchemical characterization of the inerface between $La_{0.85}Sr_{0.15}MnO_3$ and Y_2O_3-stabilized ZrO_2. *Solid State Ionics*, 1994, **70/71**, 59–64.
5. Appel, C. C., Zirconia stabilized by Y and Mn: a microstructural characterization. *Ionics*, 1995, **1**, 406–413.
6. Appel, C. C., Botton, G. A., Horsewell, A. and Stobbs, W. M., Chemical and structural changes in manganese-doped yttria stabilized zirconia studied by electron energy loss spectroscopy combined with electron diffraction. *J. Am. Ceram. Soc.*, 1999, in press.
7. Boukamp, B. A., *Equivalent Circuit*. University of Twente, The Netherlands, 1989.
8. Ikuhara, Y., Thavorniti, P. and Sakuma, T., Solute segregation at grain boundaries in superplastic SiO_2-doped TZP. *Acta Mater.*, 1997, **45**, 5275–5284.
9. Muan, A., Phase equilibriums in the system manganese oxide–silicon dioxide–air. *Am. J. Sci.*, 1959, **257**, 297–315.
10. Bonanos, N., Slotwinski, R. K., Drennan, J., Butler, P. and Steele, B. C. H., Characterisation of grain boundaries in ceramic ionic conductors using a.c. electrical techniques. *Silicates Industriels*, 1985, **9–10**, 127–132..
11. Bonanos, N., Steele, B. C. H. and Butler, E. P., Characterisation of materials. In *Impedance Spectroscopy*, ed. J. Ross Macdonald. J. Wiley & Sons, New York, 1987, pp. 215–225.